Temperature dependence of K^+-channel properties in human T lymphocytes

S. C. Lee and C. Deutsch
Department of Physiology, University of Pennsylvania, Philadelphia, Pennsylvania 19104-6085

ABSTRACT We have used whole-cell patch clamp to determine the temperature dependence of the conductance and gating kinetics of the voltage-gated potassium channel in quiescent, human peripheral blood T lymphocytes. Threshold for activation, steady-state inactivation, and the reversal potential are the same at 22° and 37°C. However, the time-constants for activation, inactivation, deactivation, and release from inactivation are quite sensitive to temperature, changing by at least a factor of five in each case over this range of temperatures. The onset of cumulative inactivation at 22° and 37°C reflects the time-course of deactivation. Peak outward current is approximately twofold greater at 37°C than at 22°C; this increase is also manifest at the single channel level. Energies of activation for conductance, activation, inactivation, deactivation, and release from inactivation are 8.2, 22.1, 25.0, 36.2, and 42.2 kcal/mol, respectively. No new channels were observed at 37°C, and there was no evidence for alteration of the K^+ conductance by putative modulators at 22 or 37°C.

INTRODUCTION

To understand the physiological role of ion channels in human T cell function and, ultimately, how they are regulated in situ, we must study the gating, conductance, kinetics, selectivity, and pharmacology of these channels at physiological temperatures. The voltage-gated K^+ channel in peripheral blood T lymphocytes produces a highly selective, delayed-rectifier current, characterized by sigmoidal, voltage-dependent activation kinetics. Under sustained depolarization, this current exhibits relatively voltage-insensitive exponential decay to an inactivated state from which recovery is slow (Cahalan et al., 1985; Deutsch et al., 1986). This voltage-gated K^+ conductance has been correlated with and may underlie normal functional responses of lymphocytes, including cytotoxic killing of foreign cells (Fukushima et al., 1984; Schlichter et al., 1986) and stimulated proliferation (DeCoursey et al., 1984; Matteson and Deutsch, 1984; Chandy et al., 1984; Deutsch et al., 1986; Lee et al., 1986). Many of these processes are sensitive to temperature in a critical way. For example, target cell lysis is inhibited at temperatures below 37°C (Engelhard et al., 1988) and antibody synthesis and secretion are both dependent on temperature (Helmreich et al., 1961; Jerne et al., 1974). Yet all of the previous work characterizing K^+ conductances in lymphocytes and monocytes has been done at room temperature (for review, see Gallin, 1986; also Choquet et al., 1987).

Address correspondence to Prof. Carol Deutsch.

We were motivated to study lymphocyte conductance at higher temperature for many reasons. First, at 37°C channel behavior and/or its biochemical regulation might be significantly different, as has been demonstrated for β-adrenergic modulation of delayed-rectifier K^+ current in guinea pig ventricular cells (Walsh et al., 1989). Second, channels that were undetectable, or labile, at 22°C might be observed at 37°C. Third, the pharmacological characteristics of the channel might be different at higher temperatures, and this would be particularly relevant to proliferation studies, which are carried out at 37°C. Fourth, information about the energetics involved in channel gating and conductance could be obtained. Hence, we studied the biophysics of the T-cell K^+ conductance at temperatures from 22° to 37°C. A preliminary report of this work has appeared previously (Lee and Deutsch, 1989). Pahapill and Schlichter (1989) have reported results similar to ours in a recent study.

METHODS

Preparation of human peripheral blood lymphocytes (PBL)

Heparinized human venous blood was collected from healthy donors. Mononuclear cells were separated by step-gradient centrifugation using a modified Ficoll-Hypaque technique, as described previously (Deutsch et al., 1986). Viability, as assessed by trypan blue exclusion, was routinely ≥95%.

Cells were used for experiments for up to 2 d after isolation. Cells not used immediately were cultured in minimal essential medium + 10%

0006-3495/90/01/49/14 $2.00

human AB serum and maintained at 37°C in humidified air + 5% CO_2.

For electrophysiological experiments, T lymphocytes were selectively adhered to 35-mm plastic Petri dishes using a panning method, as described previously (Matteson and Deutsch, 1984; Deutsch et al., 1986). PBL were incubated with a murine anti-human monoclonal antibody directed against CD2, a surface protein found on all human peripheral blood T lymphocytes (OKT11, Ortho Pharmaceutical, Raritan, NJ; or Leu 5B, Becton, Dickinson, Mountain View, CA). In some instances, we used anti-CD4 or anti-CD8 antibodies (Becton, Dickinson) to select specific subsets of the T-cell population. Cells incubated with these antibodies were then allowed to attach in the cold to dishes that had been pretreated with goat anti-mouse IgG antibody (Tago Inc., Burlingame, CA).

Electrophysiological recording

Standard patch-clamp techniques were employed, as described by Hamill et al. (1981) with application to lymphocytes (Matteson and Deutsch, 1984; Deutsch et al., 1986). We used a List Medical Electronics (Darmstadt, FRG) EPC-7 patch-clamp amplifier and a Digital Equipment Corp. (Maynard, MA) LSI 11/23 computer with a specialized interface to control voltage changes and to digitize and store data. In some instances, single-channel data were recorded with a digitizing tape system and analyzed later with the assistance of the computer. Data were low-pass filtered with the 3-kHz filter in the patch clamp or an external eight-pole Bessel filter (model 902LPF, Frequency Devices, Haverhill, MA).

Linear components of current and capacitance were subtracted, and series resistance compensation was applied to each cell in whole-cell conformation to the maximum extent possible short of uncontrolled oscillation. Uncompensated series resistance was typically 5 MΩ or less. In these experiments, the largest currents we observed were ~2 nA. Hence, in the worst case, uncompensated series resistance would have produced a 10-mV error in the clamp potential. During long sustained depolarization, there were no differences in the inactivation kinetics or reversal potential of cells with large currents compared with those with small currents, indicating that extracellular accumulation of K^+ was not a problem.

Electrodes were made of borosilicate glass (model 34500, Kimble Glass Inc., Vineland, NJ.) and coated with Sylgard 184 (Dow Corning Corp., Midland, MI). The pipette solution contained (in millimolar) 130 KF, 11 K_2EGTA, 2 $MgCl_2$, 1 $CaCl_2$, 10 HEPES, and KOH to bring the pH to 7.2 and a final osmolarity of ~280 mosmol. The bath solution was 300 mosmol at pH 7.3 and contained (in millimolar) 140 NaCl, 5 KCl, 1 $MgCl_2$, 2.5 $CaCl_2$, 5.5 glucose, 10 HEPES, and NaOH to adjust the pH. Solution osmolarity was measured with a freezing point depression osmometer (Precision Systems Osmette, Natick, MA). The bath was grounded via an agar bridge (saline at pH 7.3, no glucose, 3% [wt/vol] agar) in contact with a small reservoir that contained pipette solution. Electrical connections were made with Ag-AgCl wire.

A modified constant temperature stage (5000 KT; Micro Devices, Jenkintown, PA) was used to control the temperature of the bath. This device uses the Peltier principle and can be used for cooling as well as heating. To avoid unwanted electrical and mechanical artifacts, as well as to provide stable temperature, we used a static bath without continuous flow of solution. When working at elevated temperatures, the bath was refreshed periodically to allay the effects of evaporation. Additions and solution changes were done manually with a syringe or pipette. After attainment of the whole-cell conformation, most cells could be coaxed off the bottom of the dish. Cells in this configuration, attached only to the patch pipette, were mechanically resilient, and often withstood a number of vigorous solution changes. This also allowed us to move the cell to fixed positions in the dish where the temperature response had been calibrated. Bath temperature was monitored with a thermistor (Yellow Springs #402, Yellow Springs, OH) placed in a position comparable to that of the cell being studied. Although stable temperature gradients did exist in the dish, the temperature at the cell was known to ±0.5°C. Temperature changes were gradual: 3–4°C/min when raising temperature, and somewhat slower when lowering it.

Varying the temperature of the system may change buffering of Ca^{2+} and H^+ in the pipette solution, which could have additional effects on the K^+ conductance. HEPES is the main determinant of pipette solution pH; raising the temperature from 22° to 37°C could lower the intrapipette pH by as much as 0.20 U. At 22°C, lymphocyte K^+ conductance is very sensitive to pH in the range 7.0–7.2: a decrease in pH_i from 7.2 to 7.0 decreases peak amplitude of the current by 20%, with no effect on its kinetics. A 0.20-U change in extracellular pH would have no effect on the K^+ current (Deutsch and Lee, 1989).

In EGTA-buffered solutions, affinity of EGTA for Ca^{2+} is somewhat higher at 37°C, but a decrease of pipette solution pH to 7.0 (due to elevation of the temperature) would result in a net increase of free Ca^{2+} from 16 nM at 22°C to 30 nM at 37°C. However, our pipette solutions contain 130 mM F, which therefore sets free $[Ca^{2+}]$. Even at 37°C, the expected free Ca^{2+} concentration is < 3 nM. Intracellular free Ca^{2+} in the micromolar range has been reported to regulate the number of lymphocyte K^+ channels available to activate (Bregestovski et al., 1986; Choquet et al., 1987) and to speed inactivation (Grissmer and Cahalan, 1989). However, the small changes (in the nanomolar range) in intracellular free Ca^{2+} that may have occurred in the present experiments have not been found to affect the lymphocyte K^+ conductance (Cahalan et al., 1985).

Bath additions of β-adrenergic agonists

In order to evaluate the effect of β-adrenergic agonists, we measured whole-cell current after the following procedures: (*a*) addition of 1–2 μM prostaglandin E_2 or 0.1 mM isoproterenol at 22° or 37°C to the bathing medium of a cell already in whole-cell patch clamp; (*b*) pretreatment of cells at 22° or 37°C and subsequent patch clamp in the continued presence of 1–10 μM prostaglandin E_2 or 0.1 mM isoproterenol, with 0.1 mM and without the phosphodiesterase inhibitor IBMX; (*c*) addition of 0.1 mM of the permeant cAMP analogue CPT-cAMP to the bathing medium.

Nucleotide additions to the solution in the pipette

In order to assess the sensitivity of lymphocyte currents to nucleotides, we measured whole-cell current using the following additions to the pipette solutions: (*a*) 1 mM ATP + 0.1 mM of the permeant cAMP analogue dibutyryl-cAMP (dB-cAMP), with 0.1 mM IBMX and 0.1 mM dB-cAMP in the bath, at 22° and 37°C; (*b*) 1–5 mM ATP + 0.1–0.5 mM GTP ± 5 mM dB-cAMP, at 22° and 37°C; (*c*) 1 mM ATP ± 10–100 μM GTPγS, with or without 0.1 mM IBMX and 10 μM isoproterenol in the bath, at 22° and 37°C.

Reagents

Reagent grade chemicals from common suppliers were used wherever possible. Sources of other chemicals were as follows: Sigma Chemical

Co. (St. Louis, MO): potassium aspartate, ATP, 3-isobutyl-1-methyl xanthine (IBMX), prostaglandin E_2, isoproterenol, EGTA, and HEPES; Aldrich Chemical Co. (Milwaukee, WI): KF; Boehringer Mannheim Biochemicals (Indianapolis, IN): ATP, guanosine-5'-triphosphate (GTP), guanosine-5'-*O*-(3-thiotriphosphate) GTPγS), dibutyryl-adenosine-3':5'-monophosphate cyclic (dB-cAMP), 8-(4-chlorophenylthio)adenosine-3':5'-monophosphate cyclic (CPT-cAMP); Gibco Laboratories (Grand Island, NY): trypan blue, vitamins and amino acids for culture media.

RESULTS

Outward current at temperatures between 22° and 37°C

Fig. 1 shows the current elicited in a single T lymphocyte by depolarizing voltage steps from −70 mV to +50 mV

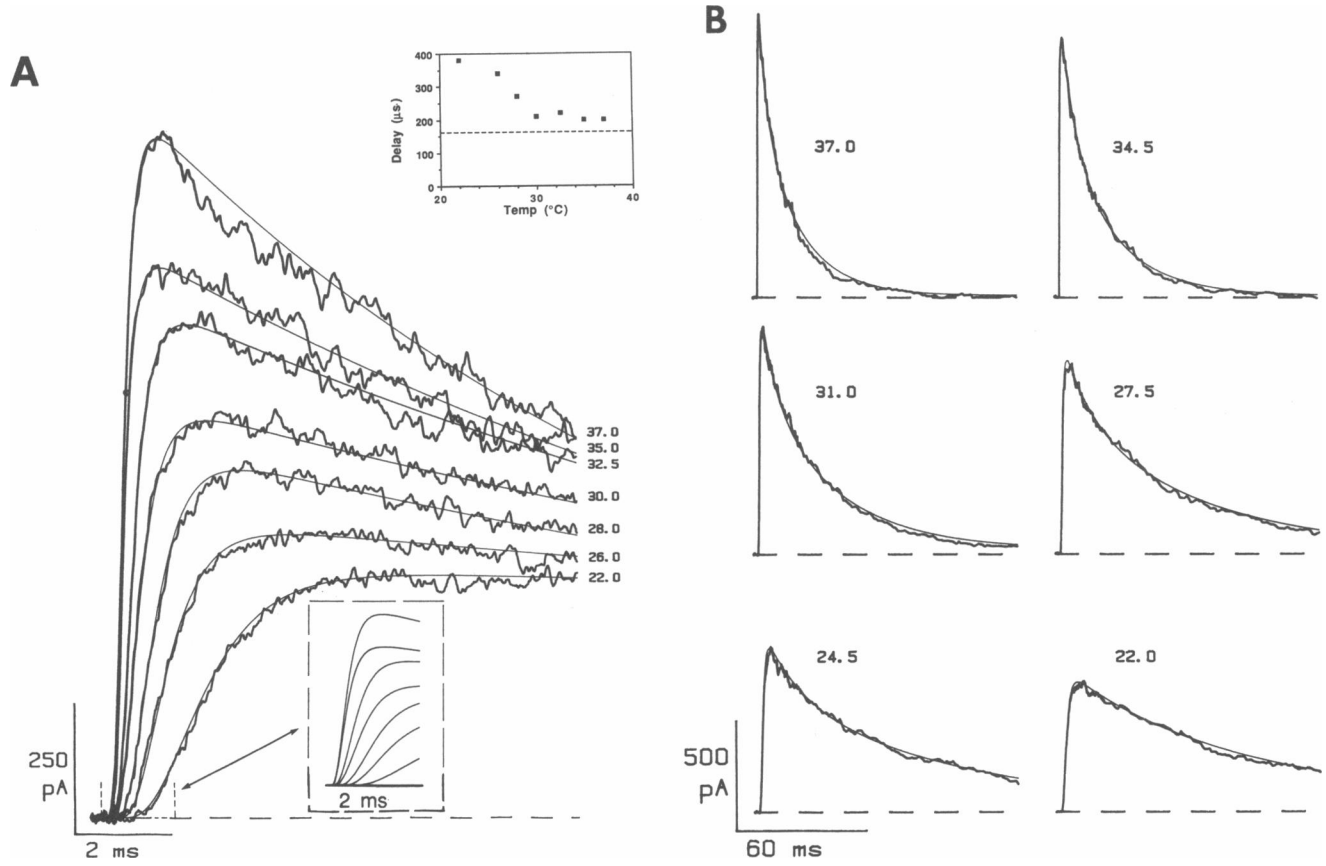

FIGURE 1 Outward current in response to a step to +50 mV at temperatures between 22 and 37°C. (*A*) These traces show the current elicited in a single cell by a depolarizing voltage step from −70 mV (first 0.20 ms of each trace) to +50 mV (remaining 9.80 ms) as bath temperature was raised from 22 to 37°C. Calculated fits were made as described in the text and are shown by the superimposed thin curves. Data were sampled at 100 kHz and filtered at 5 kHz. Linear components of current and capacitance have been subtracted. Capacitance of this cell was 1.14 pF. (*Insets*) To fit the rise in current with a consistent model at all temperatures, it was necessary to impose a delay in the calculated fits. In the lower inset, 2.0 ms of these calculated curves are redrawn beginning with the onset of the depolarization. The upper inset presents the total delay times derived from these data. Our best estimate of the (temperature-insensitive) delay inherent in the measurement system is shown by the dashed line. This delay of ~160 μs was determined as follows: by actual measurement the 50% rise time for current at the current monitor output of the EPC-7 amplifier in response to an applied voltage step from the computer was 30–40 μs; by calculation, confirmed by measurement, the 50% rise time of the Frequency Devices eight-pole Bessel filter at a cutoff frequency of 5 kHz was 100 μs; other instrumental delay was ~10 μs. Also, the calculated charging time-constant of the lymphocyte membrane was ~10 μs (7.4 μs in this example, typical of these small cells with at least partial series resistance compensation). Reasonable filtering (usually 3–10 kHz cutoff frequency) changed the total delay without affecting the shape of the current waveform. (*B*) These traces show current elicited in the same cell as in *A* by a depolarizing voltage step from −70 mV (first 2 ms of each trace) to +50 mV (remaining 120 ms) as bath temperature was lowered from 37 to 22°C. Calculated fits were derived from a model containing the sum of two exponential terms and are shown by the superimposed thin curves. Inactivation time-constants were (in milliseconds) 4.0, 18.0 for 37°C; 6.6, 23.0 for 34.5°C; 7.0, 34.0 for 31°C; 12.0, 60.0 for 27.5°C; 15.0, 85.0 for 24.5°C; and 50, 115 for 22°C, with an average fast component fraction of 0.37 (range 0.33–0.40). In all cases, a double exponential equation gave a better fit than did a single exponential equation, except for the data for 22°C, where both fits were equally good. Inactivation kinetics in this cell were particularly fast. Data were sampled and filtered at 5 kHz.

as bath temperature was raised (Fig. 1 *A*) and lowered (Fig. 1 *B*) in the range from 22° to 37°C. As the temperature of the cell was raised, peak current grew larger, and the rates of activation and inactivation became much faster (Fig. 1 *A*). These effects were reversed when the temperature was returned to 22°C; moreover, the properties of the current at intermediate temperatures did not depend on whether a particular temperature was approached from 22° or 37°C (Fig. 1 *B*).

Activation of the outward current was fit at all temperatures with a fourth power exponential of the form $[1 - \exp(t/\tau)]^4$ (Hodgkin and Huxley, 1952). Calculated sample fits (with inactivation) are shown by the superimposed thin curves in Fig. 1 *A* and described further in Fig. 2.

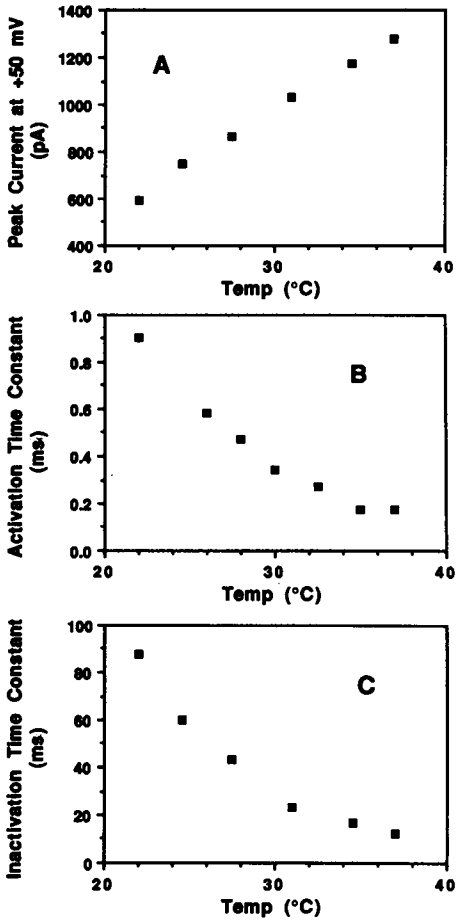

FIGURE 2 Temperature dependence of peak current, and activation and inactivation time-constants at +50 mV. This is an analysis of the current records shown in Fig. 1. (*A*) Peak current. (*B*) Activation time-constants determined as described in the text and Fig. 1. (*C*) Inactivation time-constants. For simplicity of analysis, these are best-fit single exponential time-constants for the data in Fig. 1 *B*.

To fit the initial phase of the current with a consistent model, it was necessary (and sufficient) to impose a delay in the response of the cell to the imposed voltage step (Fig. 1 *A*, *lower inset*). This delay decreased with increasing temperature (Fig. 1 *A*, *top inset*), from ~200 μs at 22°C to a limiting, very short delay at ~35°C. An uncertainty of at least ±10 μs in the measurement of these delays is due to sampling rate limitations.

In Fig. 1 *B* we employed a longer pulse protocol to more clearly define inactivation as a function of temperature. As has been demonstrated in the previous studies of this conductance, inactivation is well described by a single exponential at 22°C (Cahalan et al., 1985; Deutsch et al., 1986). However, at higher temperatures, we found that inactivation was better described by the sum of two exponentials. Both time-constants changed with temperature, with the slower time-constant being four to five times longer than the fast decay constant. Calculated fits for the data in Fig. 1 *B* are shown by the superimposed thin lines.

Peak current increased linearly with temperature, approximately doubling in the range 22° to 37°C (Fig. 2 *A* and Table 1). The change in the calculated activation time-constant was nonlinear with increasing temperature (Fig. 2 *B*), a greater percentage change occurring between 22° and 30°C than between 30° and 37°C. On average, the time-constant at 37°C was sixfold smaller than that at 22°C (Table 1). We detected no change in the activation kinetics at 37°C when we raised the cutoff frequency of our filtering; however, the insensitivity to temperature above 35°C could reflect the appearance of an instrumental limitation.

Fig. 2 *C* gives the best-fit single exponential time-constants for the inactivation data in Fig. 1 *B*. We chose a single exponential analysis because it is simple and adequate, and allows comparison with previous work. The

TABLE 1 Peak current and activation and inactivation time-constants at +50 mV at 22 and 37°C

Parameter (No. pairs)	22°	37°	Ratio 22:37*
Peak current (*pA*) ($n = 8$)	709 ± 226	1350 ± 331	0.52 ± 0.05
Activation time-constant (*ms*) ($n = 6$)	1.01 ± 0.10	0.175 ± 0.045	6.01 ± 1.34
Inactivation time-constant (*ms*) ($n = 6$)‡	139 ± 29	18.5 ± 4.9	7.68 ± 1.23

All values are given as mean ± SD.
*These ratios were calculated directly from the individual data pairs and therefore differ slightly in magnitude and have much smaller standard deviations than the values obtained using averages.
‡Best-fit single exponential model.

change in inactivation was nonlinear in a manner similar to that found for activation. On average, the time-constant at 37°C was 7.7-fold smaller than that at 22°C (Table 1).

Similar temperature-dependent alterations in K^+ conductance were observed when we selected for specific lymphocyte subtypes, CD4+ (helper phenotype) and CD8+ (suppressor phenotype).

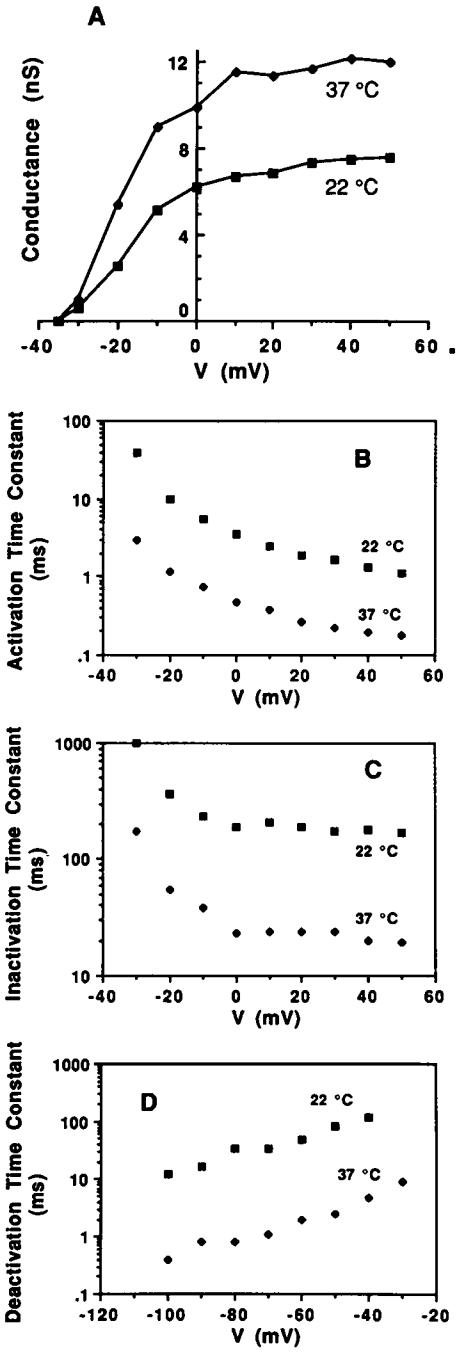

Voltage-dependence of the current and time-constants at 22° and 37°C

Figs. 1 and 2 demonstrate that the features of the K^+ conductance elicited by a standard test depolarization to +50 mV changed smoothly with temperature in the range between 22° and 37°C. Since we were primarily interested in the extremes of this range, most of our subsequent investigation compared the properties of the K^+ conductance in individual cells only at 22° and 37°C. Fig. 3 shows representative data for the voltage dependence of the properties of the current at these temperatures.

The conductance versus voltage curves at 37° and 22°C (Fig. 3 *A*) were similar with respect to steepness, midpoint (−18 and −16 mV, respectively), threshold voltage for activation (~−35 mV), and reversal potential, (−70 mV, not shown, but see below). Only the saturating level of conductance changed: it was 12 nS at 37°C and 7.5 nS at 22°C. These results demonstrate that the increase in current observed at +50 mV reflected a generalized increase in conductance with increasing temperature, with no change in voltage sensitivity.

The time-constants for activation and inactivation for the data in Fig. 3 *A* are shown in Fig. 3, *B* and *C*, respectively. Although the rates are much faster at the higher temperature, there appears to be no change in their voltage dependence. At both temperatures, as membrane potential was made more positive, the activation time-constant decreased monotonically to about the same relative extent, and the inactivation time-constant decreased to a limiting value at potentials ≥0 mV.

FIGURE 3 Voltage dependence of the conductance and time-constants for activation, inactivation, and deactivation at 22 and 37°C. The cell was stepped from a holding potential of −70 mV to the indicated membrane potential for times varying from 10 ms (to study high temperature activation) to 1.4 s (for low temperature inactivation), as required. (*A*) Conductance. Conductance is given by the ratio of peak current to driving force for K^+ at each voltage. Capacitance of this cell was 1.48 pF, and the measured reversal potential was −70 mV at both 22 and 37°C. (*B*) Activation time-constants derived from fourth power exponential fits as described in the text and Fig. 1. (*C*) Inactivation time-constants derived from single exponential fits. (*D*) Deactivation time-constants. The membrane potential was stepped from the holding potential to +50 mV for a brief period sufficient to get maximal activation of the current in this cell: 1.1 ms at 37°C and 8.0 ms at 22°C. Then the membrane potential was repolarized to the indicated potentials for 70–280 ms to monitor the decay of the current. The decay process was consistently better described by the sum of two exponentials, even at 22°C. However, we have used best-fit single exponentials here to simplify the presentation and analysis. The apparent reversal potential of the current shifted ~5 mV negative (−77 to −82 mV) in this experiment. Note that this is a different cell from *A–C*. The voltage dependence of the peak current and time-constants was the same at 22 and 37°C.

Deactivation is the rate of decay of current upon repolarization after a current-inducing depolarization. This is shown in Fig. 3 *D*. There was no change in the voltage sensitivity of the rate of decay, despite a large increase in the rate at 37°C. At −60 mV, the best-fit single exponential time-constant for the decay was 41.9 ± 7.9 ms at 22°C and 2.1 ± 0.2 ms at 37°C (n = 2), for an increase in relative rate of 20.8 ± 6.0.

In most experiments the apparent reversal potential was insensitive to temperature. This was probably the result of counterbalancing effects. With no change in channel selectivity, the Nernst potential for K^+ should shift ~5 mV more negative as the temperature is raised from 22° to 37°C. This was occasionally observed, as in the cell used for Fig. 3 *D*, where the reversal potential shifted from ~−77 to −82 mV. We also observed an erratic 2–5-mV positive offset of the potential of a patch electrode with its tip in the bath solution as the bath temperature was raised from 22° to 37°C, which would give an apparent negative shift in reversal potential. Since we usually saw no shift in the reversal potential, this suggests that the actual reversal potential shifts a few millivolts positive at higher temperature. More experiments are necessary to clarify this issue.

In summary, the voltage dependence of the peak current and time-constants was the same at 22° and 37°C.

Steady-state inactivation

Steady-state inactivation describes the modulation of maximum current observed as a function of the holding potential of the cell. In no case, using our usual protocol (see below), did we observe significant decrease of peak current until the holding potential was ~10 mV negative to the observed threshold potential in that cell, and then the decrease in current with further depolarization was very rapid. The shape and position of the steady-state inactivation curve did not change as temperature was raised from 22° to 37°C.

To determine steady-state inactivation we typically began by clamping the cell at a hyperpolarized holding potential (−90 or −100 mV) for a number of minutes. We assayed the peak current with short depolarizing voltage steps to +50 mV spaced at least 1 min apart until a stable peak current was obtained. The holding potential was then set 10 mV positive from the last, and the cell was held there for at least 90 s before the next test voltage step was applied. The development of a stable decreased peak current (i.e., steady-state inactivation) sometimes required a number of minutes. On the other hand, peak current assayed as the cell is repolarized from a long, sustained depolarization may lead to an overestimate of the amount and the voltage dependence of steady-state inactivation because the release from inactivation is voltage dependent and very slow. Hence, the manner in which the measurement is performed can potentially affect the apparent dependence of steady-state inactivation on voltage.

Release from inactivation

Release from inactivation is the recovery of peak current as a function of time after a maximal inactivation. Release from inactivation as a function of temperature is shown in Fig. 4.

At 37°C this process was much faster than at 22°C (Fig. 4 *B*). Using best-fit single exponentials, the recovery time-constant at −90 mV was 18.4 ± 3.3 s and 0.57 ± 0.10 s at 22° and 37°C, respectively (n = 3, ± SD). The time-course of recovery of the current was somewhat better fit by the sum of two exponentials, but both time-constants changed proportionally with temperature. The ratio of single-exponential time-constants (τ22°C:τ37°C) for these three data pairs is 32.7 ± 2.6. When the membrane potential was held at −70 mV, the recovery time-constant at 37°C was ~50% longer than at −90 mV; at 22°C it was more difficult to determine, but it was probably more than 50% longer.

Cumulative inactivation

Cumulative inactivation, defined by Aldrich et al. (1979) as a smaller peak current during one pulse in a train compared with the current at the end of the preceding pulse, is characteristic of the lymphocyte voltage-gated conductance (Matteson and Deutsch, 1984; DeCoursey et al., 1984). The sensitivity of this response to temperature is shown in Fig. 5 as a function of the interpulse interval. Fig. 5 *A* shows the pulse trains that gave maximal cumulative inactivation (the ratio of peak current in the second step to peak current in the first step) in this cell at 22° and 37°C. Fig. 5 *B* shows the dependence of cumulative inactivation on the interval between pulses. At both 22° and 37°C, the kinetics of onset of cumulative inactivation and of recovery from cumulative inactivation are qualitatively similar to those described by Aldrich et al. (1979) for cumulative inactivation of a K^+ current in molluscan neuron. At 22°C, maximal cumulative inactivation was 34 ± 5% (n = 3, ± SD) for an interpulse interval of 50–100 ms. At 37°C, maximal cumulative inactivation was 18 ± 3% (n = 3, ± SD) for an interpulse interval of 1.0–2.0 ms. Cumulative inactivation did not occur if the interpulse interval was longer than 1–2 s at 37°C, but significant inactivation was still observed at 22°C with an interpulse interval of 20 s.

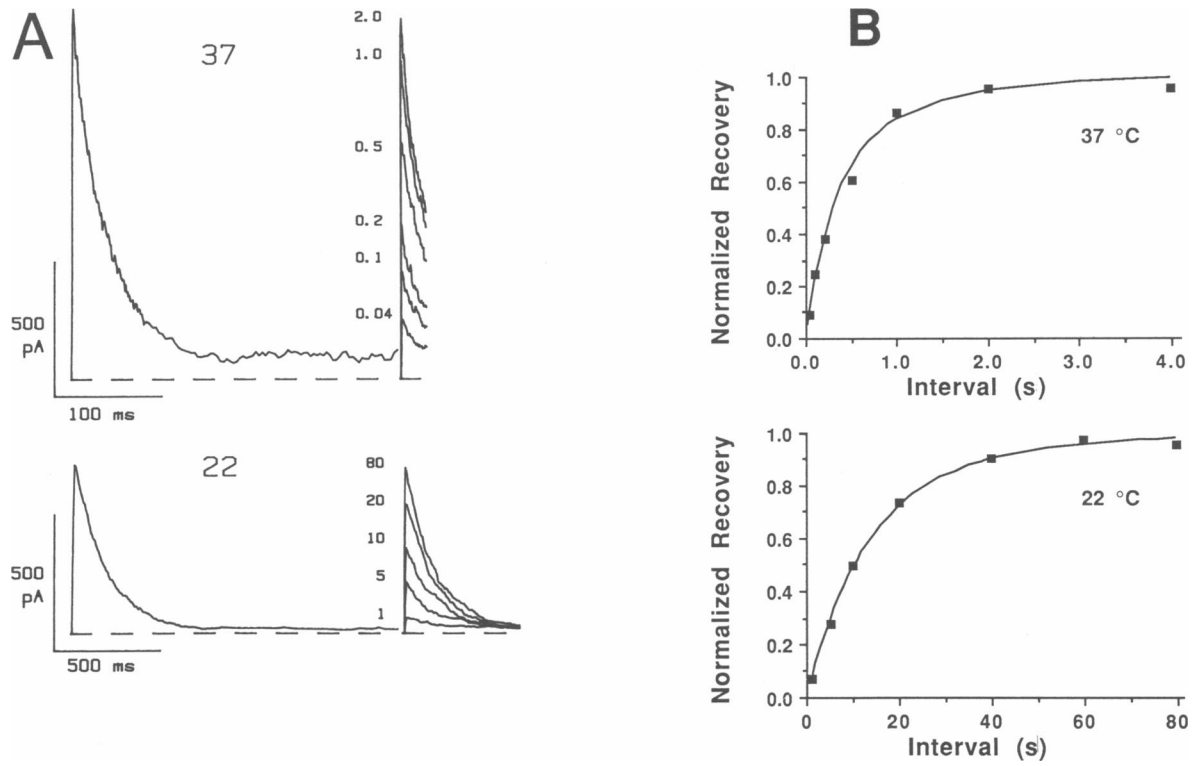

FIGURE 4 Release from inactivation. (*A*) Peak current recovery after inactivation. In this cell, the membrane potential was stepped from −90 mV to +50 mV for 1.548 s (22°C) or 304.8 ms (37°C), repolarized to −90 mV for varied intervals, and then depolarized again to +50 mV to assay recovery of peak current from inactivation. We chose the length of the inactivating depolarization at each temperature such that the current was at its plateau value for about the same proportion of the data record. We used a holding potential of −90 mV in these experiments because full recovery of the current at 22°C using a holding potential of −70 mV was impractically slow (>2 min). The interval between each trial was 115 s (22°C) or 40 s (37°C). Sampling rate was 166.7 Hz (22°C) or 1,667 Hz (37°C). These current records were not leak subtracted. Capacitance of this cell was 1.66 pF. (*B*) Fractional peak current as a function of the repolarization interval for the data in *A*. In this analysis, we considered the relevant, inactivating current to be that greater than the steady-state current level; i.e., we subtracted the height of the plateau from the peak of both currents before normalizing. The data were somewhat better fit with the sum of two exponentials. The fit lines were generated with time-constants of 11.8 and 29.0 s, fast fraction 0.70 (22°C), and 0.28 and 1.0 s, fast fraction 0.61 (37°C).

Single-channel currents as a function of temperature

Single-channel currents were recorded from the outside-out patch or whole-cell configurations. Although excised patches are superior for observing unitary events of voltage-gated channels, our experience has been that excised patches with small numbers of channels are very difficult to obtain with these cells. In this study, our two best examples of outside-out patches with only two or three channels are shown in Fig. 6. The unitary currents elicited by a 100-ms voltage step from the holding potential to 0 or +50 mV increased in size as the temperature was raised from 22° to 37°C. On average, the sizes of the most prevalent unitary currents were 14.1 ± 0.6 pS (n = 6, ± SD) and 26.2 ± 1.5 pS (n = 6, ± SD) at 22° and 37°C, respectively.

Single-channel currents in lymphocytes are readily obtained by recording residual activity in whole-cell configuration during a sustained depolarization (Cahalan et. al., 1985). Fig. 7 shows an example. There are many more, but briefer, channel openings at 37° than at 22°C. There was also a suggestion of a slow decline in channel activity, which may reflect population of a second inactivation state from which recovery, upon repolarization, is very slow (see also Cahalan et al., 1985).

Activation energies

The time-constants obtained for the kinetic processes described above can be used to calculate the heat of activation involved in the transition from one channel state to another, according to the Arrhenius equation:

$$k = A \exp(-E_a/RT),$$

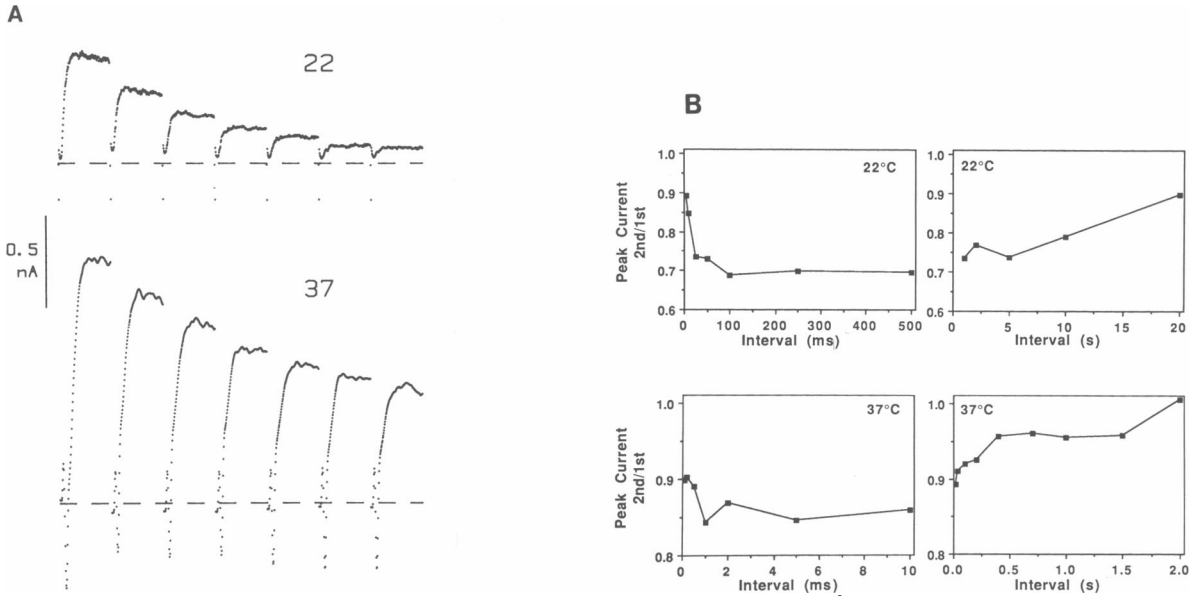

FIGURE 5 Cumulative inactivation at 22° and 37°C. (*A*) A cell in whole-cell configuration was stepped repetitively from a holding potential of −90 mV to +50 mV with intervals of varied durations between the steps. The step length was chosen to give maximal activation of current with little obvious inactivation; the step length was 14.0 ms at 22°C and 1.4 ms at 37°C. The interpulse duration was 100 ms for the data shown at 22°C and 2.0 ms for the data at 37°C. The interpulse currents are not shown. Linear components of capacitance and current were not subtracted. Cell capacitance was 1.11 pF. Data at 22°C were collected at a sampling rate of 10 kHz with a 3-kHz filter; data at 37°C were collected at 100 kHz with a 5-kHz filter. (*B*) Currents were elicited in response to repetitive voltage steps by the procedure shown in *A* for interpulse intervals of 5 ms to 20 s at 22°C and 0.1 ms to 2.0 s at 37°C. The ratio of peak current in the second current trace of the train vs. that in the first current trace was taken as a measure of cumulative inactivation (after Aldrich et al., 1979). These data were not corrected for holding current at −90 mV or for the noninactivating residual current at the end of a long depolarization, as each of these was <1% of peak current.

where k is the rate constant for the transition, A is the frequency factor related to the underlying vibrational frequency and the entropy of the transition state, E_a is the activation energy (heat of activation in the Eyring formulation), and R is the gas constant. The temperature dependence of reaction rates depends mostly on the enthalpic, rather than the entropic, component. Fig. 8 shows representative Arrhenius curves obtained by linear regression of the data from Fig. 2. Shown are whole-cell conductance (Fig. 8 *A*), activation (Fig. 8 *B*), and inactivation (Fig. 8 *C*). The slope of the regression line in such a plot is equal to E_a/R.

A summary of the calculated activation energies for activation, inactivation, deactivation, and conductance are given in Table 2. The values range from 42 kcal/mol for release from inactivation to 8 kcal/mol for K^+ conductance.

Putative modulators of the K^+ conductance

An important additional goal of this study was to search at 37°C for other channels (voltage-, ligand-, and/or second messenger-gated) that might have been nonfunctional or undetectable at room temperature. The existence of such channels has been implicated by indirect measurements of agonist- and Ca^{2+}-induced membrane hyperpolarization and volume changes in lymphocytes (Wilson and Chused, 1985; Grinstein and Dixon, 1989). Also, we wished to reinvestigate whether cAMP could be a modulator of the voltage-gated K^+ current in lymphocytes, as has been reported (Choquet et al., 1987; Lee et al., 1988). In our previous study of quiescent human T cells at room temperature, we had been unable to detect any effect of cAMP or cAMP-modulating agents on the outward current (Krause et al., 1988). However, there is precedence for a temperature-sensitive, cAMP-mediated effect on K^+ conductance in a cardiac cell (Walsh et al., 1988, 1989), so it seemed worthwhile to reinvestigate this issue at higher temperature.

As we varied temperature from 22° to 37°C we found no new channels, nor were any consistent effects on peak current or gating kinetics of the whole-cell, voltage-gated K^+ conductance observed upon additions of β-adrenergic agonists (prostaglandin E_2 or isoproterenol), cAMP analogues, or nucleotides to the bath or pipette solutions (see

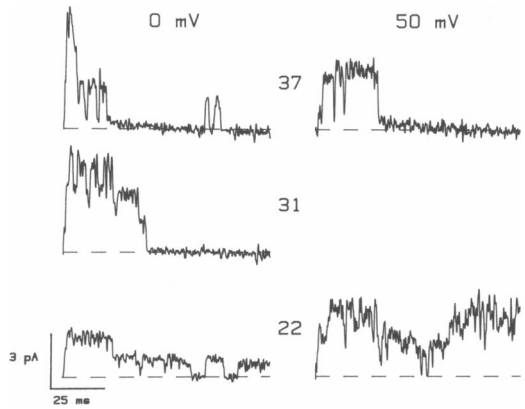

FIGURE 6 Voltage-gated single-channel currents in excised outside-out patches. Each trace shows the current recorded at the indicated temperatures in response to a 100-ms voltage step to 0 mV or +50 mV from a holding potential of −70 mV. The data at 0 mV and +50 mV were obtained from different cells. The patch, which was stepped to 0 mV, contained at least three channels; the patch, which was stepped to +50 mV, apparently had two channels, but only one was seen after the temperature was raised to 37°C. The sampling rate was 10 kHz, and the data were filtered at 1 kHz. Calculated single-channel conductance was 14.6 and 10.7 pS at 22°C, 23.3 pS at 31°C, and 29.1 pS at 37°C for the data obtained at 0 mV; and 14.8 pS at 22°C, and 25.5 pS at 37°C for the data obtained at +50 mV. These data records were adjusted so that the closed state shows as zero current; and the initial capacitive artifact was subtracted using models derived from records in which no channels opened.

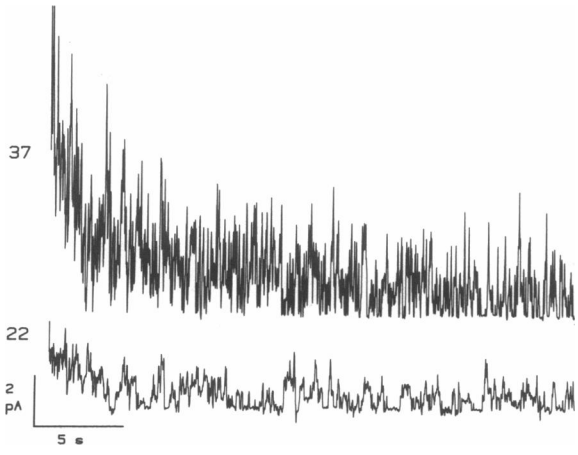

FIGURE 7 Single-channel currents in whole-cell configuration. These records show 30 s of single-channel activity in a whole cell at 22° and 37°C. The records begin 1 s after the membrane was depolarized from −90 to 0 mV. These data are not leak corrected. Capacitance of this cell was 1.58 pF, and its peak current at +50 mV, 22°C was 375 pA. Single-channel activity decreased with time after depolarization.

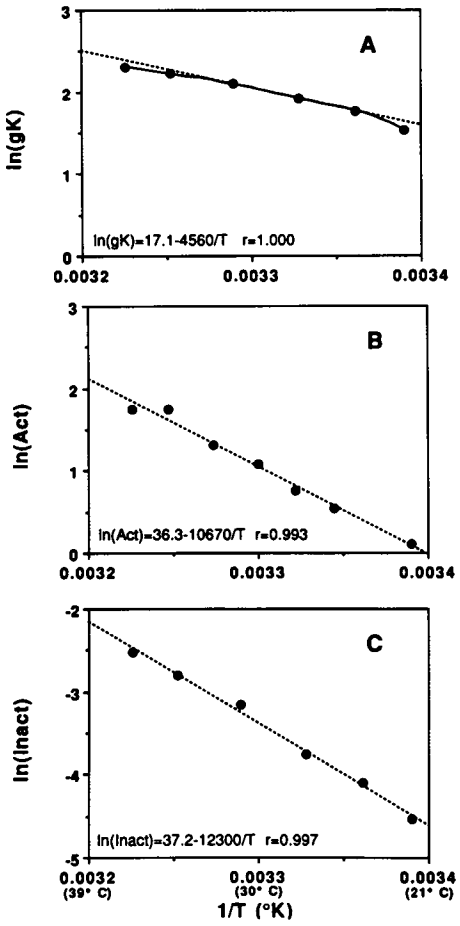

FIGURE 8 Arrhenius plots for whole-cell conductance and activation and inactivation time-constants. Curves were obtained by linear regression of the data shown in Fig. 2. The slope is equal to E_a/R, where E_a is the activation energy and R the gas constant. r is the correlation coefficient. (*A*) Whole-cell conductance. For this data, E_a (gK) was 9.1 kcal/mol, determined by a fit through the linear central portion of the curve. The slight nonlinearity in the complete curve may arise from inaccuracy in the determination of peak current. Factors which could affect the measurement of peak current or its analysis include: (*a*) the greater percentage change, on average, in the rate of inactivation than in the rate of activation in going from 22 to 37°C (Table 1) could decrease the expected peak current at 37°C by ~5%; (*b*) uncertainty in the reversal potential at 37°C which might lead to a ~5% underestimate of calculated conductance if there were a shift to more positive voltage; (*c*) incomplete series resistance compensation, which would decrease the calculated conductance at all temperatures, but which could lead to as much as a 5% additional error at high temperatures because of the larger currents; (*d*) by far the largest factor, the decrease of pipette solution pH expected to occur as the temperature is raised could lower peak current by as much as 20% at 37°C (see Methods). (*B*) Activation time-constant. E_a (act) was 21.2 kcal/mol. (*C*) Inactivation time-constant. E_a (inact) was 24.4 kcal/mol.

TABLE 2 Energies of activation

Process	Energy	Q_{10} (27–37°C)
	kcal/mol	
Conductance (n = 8)	8.2 ± 1.2	1.56
Activation (n = 6)	22.1 ± 3.4	3.31
Inactivation (n = 6)	25.0 ± 1.5	3.87
Deactivation (n = 2)	36.2 ± 5.9	7.09
Release from inactivation (n = 3)	42.2 ± 1.0	9.81

Energy values (E_a) were calculated from the slope of the regression lines of ln τ vs. T^{-1} for the temperature range 22–37°C, as exemplified by Fig. 8. The slope equals E_a/R, where R, the gas constant, is 1.9872 caldeg^{-1}mol^{-1}. Q_{10} values were calculated by evaluating exp{$(E_a/R)[(1/300)-(1/310)]$}. Values of E_a are given as mean ± SD.

Methods). Also, there was no detectable change in on-cell K^+ current when the temperature was raised from 22° to 35°C in the presence of 1 μM prostaglandin E_2.

Most of the nucleotide experiments were done using a pipette solution made with potassium aspartate rather than KF. When ATP was added to the aspartate solution, we sometimes observed a small, non–voltage-gated current, consistent with the anion conductance discovered under similar conditions by Cahalan and Lewis (1988). This current was seen with and without GTPγS in the pipette, and at 22° and 37°C. It was, however, seen infrequently, probably because consistent activation of the current occurs when the pipette solution is hypertonic (Cahalan and Lewis, 1988), and our pipette solutions were slightly hypotonic.

Often, but not consistently, we found that average peak current was less in intact cells placed into whole-cell patch-clamp configuration during the first 30 min after addition of prostaglandin E_2 to the bath at 37°C. It was more difficult to obtain high resistance seals during this treatment, so that the smaller currents could represent artifacts.

There were also no detectable effects of the mitogen phytohaemagglutinin (PHA-P, 0.7–1.3 μg/ml) at 37°C in whole-cell or on-cell configurations.

DISCUSSION

Temperature has profound effects on the properties of the voltage-gated K^+ conductance of human T cells. Current kinetics are faster and amplitude larger at higher temperatures. However, the reversal potential of the current, threshold for activation, and voltage sensitivity of gating are not affected by temperature between 22° and 37°C.

Conductance

On average, whole-cell conductance increased by a factor of 1.92 ± 0.20 in going from 22° to 37°C (Table 1), corresponding to an activation energy of 8.2 kcal/mol. Although we have calculated the temperature dependence as an energy of activation (E_a), a one-barrier Eyring model is not implied. We chose to represent our results in this fashion in order to convey the overall magnitude of the energy barriers involved in the process of ion flow. This is a best estimate of E_a, inasmuch as the Arrhenius plot of whole-cell conductance is slightly nonlinear (Fig. 8 *A*).

By direct measurement, we found a 40% increase in conductance of the patch-clamp system with an open-tipped pipette in the bath as the temperature was raised from 22° to 37°C, which is equivalent to a process that has an activation energy of 4.1 kcal/mol. This is the change expected from the increased conductivity of K^+, Na^+, and Cl^-. However, in this study, and similar to other determinations of K^+ conductance (compare Q_{10} values in Table 2 with those in Table 3) the activation energy of conductance was twice that of ion flow in free solution. This implies that K^+ permeation through the open channel is not equivalent to unrestricted aqueous diffusion.

Another factor that could contribute to the increase in whole-cell conductance is that more channels open at higher temperature and/or open more quickly or more often. There may also be an increased preference for the larger conductance state of the channel at higher temperature. Nevertheless, we found that the size of the single-channel currents increased by a factor of 1.86 ± 0.07 from 22° to 37°C, which is not statistically different from the increase in the macroscopic current. These data suggest that the increase in macroscopic peak current can be accounted for completely by an equivalent increase in the size of the underlying unitary currents.

Activation and inactivation kinetics

The energy barriers (E_a) for K^+ current activation and inactivation are ~20–25 kcal/mol, corresponding to an increase in rate of about sevenfold from 22° to 37°C. Although E_a for inactivation was generally higher than E_a for activation, they were not statistically different. These activation energies are at the high end of the range of those found previously for other K^+ conductances (compare Q_{10} values in Table 2 with those in Table 3).

Activation of the lymphocyte K^+ current displays a temperature-sensitive delay (Fig. 1). A similar delay has been reported for activation of rat muscle K^+ currents (Pappone, 1980; Beam and Donaldson, 1983). The kinetic scheme that Beam and Donaldson (1983) use to describe

TABLE 3 Q_{10} values for K^+ channel gating kinetics and conductance

Preparation	Act	Deact	Conductance	Temp	Ref
				°C	
Delayed rectifier					
Nodes of Ranvier					
(*Xenopus laevis*)	3.2	2.8	1.2	2–20	*a*
Guinea pig ventricle	—	2.0	2.1	22–33	*b*
Squid axon					
(*Loligo forbesi*)	~3	—	1.0–1.5	6–22	*c*
Rat skeletal muscle	2	—	1.4*	30–38	*d*
	6	—		<8.7	
	2.5	—	—	10–20	*e*
Ca^{2+}-activated					
Embryonic rat myotube	—	—	~1.4	22–32	*f*
Anomalous rectifier					
Tunicate egg cell					
(*Halocynthia aurantium*)	—	—	1.5	2–20	*g*

*Temperature range for this determination was 6.8–32.4°C. (*a*) Frankenhaeuser and Moore, 1963; (*b*) Walsh et al., 1989; (*c*) Hodgkin et al., 1952; (*d*) Beam and Donaldson, 1983; (*e*) Pappone, 1980; (*f*) Barrett et al., 1982; (*g*) Fukushima, 1982.

muscle K^+ currents is adequate in most respects to describe the features of the lymphocyte K^+ conductance. However, in contrast to their model and that of Aldrich (1981), we have no evidence that K^+ channel inactivation in the lymphocyte occurs from a closed state (see discussion of cumulative inactivation below).

A second exponential component was required in order to fit the time-course of inactivation for lymphocytes depolarized at 37°C. This suggests that there are at least two inactivation states, with possibly different sensitivity to temperature. An alternative explanation is that fast channel closure to a noninactivated state and fast reopening occurs, and is more prevalent at the higher temperature (as suggested by Fig. 7).

Deactivation and release from inactivation

Deactivation and release from inactivation proved to be much more sensitive to temperature than the other properties that we studied, with activation energies on the order of 35–40 kcal/mol. The large E_a for release from inactivation may reflect energy barriers involved in a direct pathway from the inactivated state to the closed state and/or a pathway from the inactivated state to the closed state via an open state. The latter case might be analogous to Armstrong's proposed mechanism for inactivation, which involves block of the open channel by an inactivation "particle" (Armstrong, 1969). In this model, release from inactivation would require removal of the blocking particle from the channel, after which the channel would close (deactivate). The observed voltage sensitivity for the release from inactivation might be conferred by movement of charge during any processes involved in these pathways and/or by inward movement of K^+ at hyperpolarized potentials, displacing the inactivation particle from the channel.

Cumulative inactivation

As with the other properties of the lymphocyte K^+ conductance, both the onset of and recovery from cumulative inactivation were much faster at higher temperatures. As has been described for the delayed K^+ current of molluscan neuron (Aldrich et al., 1979), cumulative inactivation in the lymphocyte exhibited a U-shaped dependence on the time between voltage steps, and the onset of cumulative inactivation reflected the time-course of current deactivation upon repolarization at each temperature. Aldrich and colleagues (1979, 1981) attribute cumulative inactivation to a combination of fast inactivation from a closed state and slow recovery from an inactivated state. This model depends on the fact that the time constants for activation and fast inactivation are comparable in the molluscan neuron. In the lymphocyte, recovery from inactivation is also very slow, but the rate of activation of the K^+ current is two orders of magnitude faster than the observed rate of inactivation. Hence, a different model may apply in the case of the lymphocyte.

We think that cumulative inactivation could result from ordinary inactivation of open channels during the time in which deactivation is occurring. The following arguments support this hypothesis. Deactivation can be described by an exponential decay with time-constant τ_{deact}. The integral of current during deactivation is $\tau_{deact} \times$ number of initially open channels $\times$ channel conduc-

tance driving force. The number of channels open upon repolarization (beginning of deactivation) is equal to the number of open channels at the end of the depolarization step. When the interpulse interval is long compared with τ_{deact} but still short compared with the rate of release from inactivation, all of these channels are open for an average time equal to τ_{deact}, and recovery from inactivation is insignificant during the interpulse interval. For the data in Fig. 5, the deactivation time-constant at 22°C and −90 mV was ~30 ms, the inactivation time-constant at +50 mV was ~210 ms, and the decrease in peak current from the first current trace to the second was ~30%. The time-constant, τ, for inactivation in the interpulse interval would be given by $\exp[-(14/210) - (30/\tau)] = 0.7$, where 14 ms was the total time the membrane was at +50 mV during the period between the peak of the first current trace and the peak of the second (10 ms at the end of pulse 1, plus 4 ms at the beginning of pulse 2). This expression yields $\tau = 103$ ms, approximately twice as fast as inactivation at positive potentials. Because the time-constant for release from inactivation was ~20 s, <1% of channels inactivated during the 100-ms interpulse interval would be expected to recover. At 37°C a similar calculation, using the expression $\exp[-(1.4/28) - (1.45/\tau)] = 0.85$, yields $\tau = 12.9$ ms. Release from inactivation in the 2-ms interpulse interval would be only 1%. Hence, the time-constant describing this faster inactivation has the same temperature sensitivity as conventional inactivation, i.e., an eightfold change at 37° compared with 22°C. However, maximal cumulative inactivation is less at 37° than at 22°C, because the amount of time that channels are open during deactivation is disproportionately less (20-fold change at 37° versus 22°C). Fast inactivation of the K^+ channel at hyperpolarized potentials could be the result of the increased driving force for entry of extracellular Ca^{2+} into the open channel. Inactivation of the T cell K^+ channel has been shown to be sensitive to both intracellular and extracellular Ca^{2+}, and there is evidence to suggest that at least part of the inactivation process may be due to Ca^{2+} entry and slow permeation through the K^+ channel (Grissmer and Cahalan, 1989).

In summary, the energies of activation for gating of the human T lymphocyte K^+ channel are often higher than those found for other ion channels, while the energy of activation for the conductance of K^+ through this channel is similar to that for other channels. These high energy barriers may reflect any or all of the following: (*a*) metabolic (biochemical) processes that regulate these channels; (*b*) dielectric properties of the lymphocyte membrane and/or this channel (Parsegian, 1969); (*c*) lipid–protein steric constraints in the lymphocyte membrane.

Biological significance

What regulates the K^+ channel in situ? Ligands and second messengers do not gate this channel, although some can modulate its conductance and kinetics. For example, in T cells mitogenic lectins can change the voltage sensitivity (Cahalan et al., 1985; DeCoursey et al., 1985) and intracellular pH and Ca^{2+} can modulate conductance and inhibit channel opening, respectively (Deutsch and Lee, 1989; Bregestovski et al., 1986). In B lymphocytes, modulation by cAMP, cGMP, and Ca^{2+} has been demonstrated (Choquet et al., 1987, 1988). To date, only voltage has been shown to gate this channel. The resting membrane potential of the human T cell is ~−70 mV (Deutsch et al., 1979; Wilson and Chused, 1985). Except for an osmotically sensitive electrogenic Cl^- permeability (Grinstein et al., 1982; Cahalan and Lewis, 1988), there is no demonstrated mechanism to depolarize the membrane and gate the K^+ conductance.

One motivation for this study was to search for biochemical and electrical modulators of K^+ channel function under physiological conditions. We did not find any new conductances at 37°C, nor did we discover any biochemical pathway by which the lymphocyte could modulate K^+ channel function. Another reason for studying the K^+ conductance at 37° comes from observations that K^+ channel antagonists inhibit mitogen-induced T cell proliferation (Deutsch et al., 1986; Chandy et al., 1984; Price et al., 1988) and cytotoxic killing (Schlichter et al., 1986). Because these processes and their inhibition occur at 37°C, it was important to determine the effect of some representative K^+ channel blockers at 37°C. In preliminary experiments we have found that charybdotoxin, tetraethylammonium, and quinine are equipotent at 22° and 37° C (Lee and Deutsch, unpublished data).

This study of lymphocytes at different temperatures has demonstrated some interesting properties of the T cell K^+ conductance. Specifically, deactivation and recovery from inactivation are remarkably temperature-dependent compared with activation and inactivation. Thus, K^+ current properties are not simply scaled up or down by temperature, but these processes occur differently in relation to each other at different temperatures. Perhaps most significantly, inactivation would appear to be a much less important factor in any model of T cell function because release from inactivation at 37°C occurs on a time-scale of seconds instead of minutes. This means there are more channels available to open at any given time, at all voltages.

Though we have not yet found any temperature dependence of hormones, putative second messengers, pharmacological agents, or the presence of new channels, lym-

phocyte electrophysiology is in its infancy and many possibilities are yet to be explored. One such possibility is that elevated temperature (i.e., fever) can modulate immunoresponsiveness of T cells by altering the kinetics of channel gating.

Charybdotoxin was a kind gift of Prof. Chris Miller (Brandeis University).

This work was supported by National Institutes of Health grant GM 41467.

Received for publication 17 April 1989 and in final form 21 August 1989.

REFERENCES

Aldrich, R. W. 1981. Inactivation of voltage-gated delayed potassium current in molluscan neurons. A kinetic model. *Biophys. J.* 36:519–532.

Aldrich, R. W., P. A. Getting, and S. H. Thompson. 1979. Inactivation of delayed outward current in molluscan neurone somata. *J. Physiol. (Lond.).* 291:507–530.

Armstrong, C. M. 1969. Inactivation of the potassium conductance and related phenomena caused by quaternary ammonium ion injection in squid axons. *J. Gen. Physiol.* 54:553–575.

Barrett, J. N., K. L. Magleby, and B. S. Pallotta. 1982. Properties of single calcium-activated potassium channels in cultured rat muscle. *J. Physiol. (Lond.).* 331:211–230.

Beam, K. G., and P. L. Donaldson. 1983. A quantitative study of potassium channel kinetics in rat skeletal muscle from 1 to 37°C. *J. Gen. Physiol.* 81:485–512.

Bregestovski, P., A. Redkozubov, and A. Alexeev. 1986. Elevation of intracellular calcium reduces voltage-dependent potassium conductance in human T cells. *Nature (Lond.).* 319:776–778.

Cahalan, M. D., and R. S. Lewis. 1988. Role of potassium and chloride channels in volume regulation by T lymphocytes. *In* Cell Physiology of Blood. R. B. Gunn and J. C. Parker, editors. Rockefeller University Press, New York. 281–301.

Cahalan, M. D., K. G. Chandy, T. E. DeCoursey, and S. Gupta. 1985. A voltage-gated potassium channel in human T lymphocytes. *J. Physiol. (Lond.).* 358:197–237.

Chandy, K. G., T. E. DeCoursey, M. D. Cahalan, C. McLaughlin, and S. Gupta. 1984. Voltage-gated potassium channels are required for human T lymphocyte activation. *J. Exp. Med.* 160:369–385.

Choquet, D., and H. Korn. 1988. Dual effects of serotonin on a voltage-gated conductance in lymphocytes. *Proc. Natl. Acad. Sci. USA.* 85:4557–4561.

Choquet, D., P. Sarthou, D. Primi, P.-A. Cazenave, and H. Korn. 1987. Cyclic AMP-modulated potassium channels in murine B cells and their precursors. *Science. (Wash. DC).* 235:1211–1214.

DeCoursey, T. E., K. G. Chandy, S. Gupta, and M. D. Cahalan. 1984. Voltage-gated K^+ channels in human T lymphocytes: a role in mitogenesis? *Nature. (Lond.).* 307:465–468.

DeCoursey, T. E., K. G. Chandy, S. Gupta, and M. D. Cahalan. 1985. Voltage-dependent ion channels in T-lymphocytes. *J. Neuroimmunol.* 10:71–95.

Deutsch, C., and S. C. Lee. 1989. Modulation of K^+ currents in human lymphocytes by pH. *J. Physiol. (Lond.).* 413:399–413.

Deutsch, C. J., A. Holian, S. K. Holian, R. P. Daniele, and D. F. Wilson. 1979. Transmembrane electrical and pH gradients across human erythrocytes and human peripheral lymphocytes. *J. Cell. Physiol.* 99:79–94.

Deutsch, C., D. Krause, and S. C. Lee. 1986. Voltage-gated potassium conductance in human T lymphocytes stimulated with phorbol ester. *J. Physiol. (Lond.).* 372:405–423.

Engelhard, V. H., J. R. Gnarra, J. Sullivan, G. L. Mandell, and L. S. Gray. 1988. Early events in target-cell lysis by cytotoxic T cells. *Ann. NY Acad. Sci.* 532:303–313.

Frankenhaeuser, B., and L. E. Moore. 1963. The effect of temperature on the sodium and potassium permeability changes in myelinated nerve fibres of *Xenopus laevis*. *J. Physiol. (Lond.).* 169:431–437.

Fukushima, Y. 1982. Blocking kinetics of the anomalous potassium rectifier of tunicate egg studied by single channel recording. *J. Physiol. (Lond.).* 331:311–331.

Fukushima, Y., S. Hagiwara, and M. Henkart. 1984. Potassium current in clonal cytotoxic T lymphocytes from the mouse. *J. Physiol. (Lond.).* 351:645–656.

Gallin, E. K. 1986. Ionic channels in leukocytes. *J. Leukocyte Biol.* 39:241–254.

Grinstein, S., and S. J. Dixon. 1989. Ion transport, membrane potential, and cytoplasmic pH in lymphocytes: changes during activation. *Physiol. Rev.* 69:417–481.

Grinstein, S., C. A. Clarke, and A. Rothstein. 1982. Increased anion permeability during volume regulation in human lymphocytes. *Philos. Trans. R. Soc. Lond. B. Biol. Sci.* B299:509–518.

Grissmer, S., and M. D. Cahalan. 1989. Divalent ion trapping inside potassium channels of human T lymphocytes. *J. Gen. Physiol.* 93:609–630.

Hamill, O. P., A. Marty, E. Neher, B. Sakmann, and F. J. Sigworth. 1981. Improved patch-clamp techniques for high-resolution recording from cells and cell-free membrane patches. *Pfluegers Arch. Eur. J. Physiol.* 391:85–100.

Helmreich, E., M. Kern, and H. N. Eisen. 1961. The secretion of antibody by isolated lymph node cells. *J. Biol. Chem.* 236:464–473.

Hodgkin, A. L., and A. F. Huxley. 1952. A quantitative description of membrane current and its application to conduction and excitation in nerve. *J. Physiol. (Lond.).* 117:500–544.

Hodgkin, A. L., A. F. Huxley, and B. Katz. 1952. Measurement of current-voltage relations in the membrane of the giant axon of *Loligo*. *J. Physiol. (Lond.).* 116:424–448.

Jerne, N. K., C. Henry, A. A. Nordin, H. Fuji, A. M. C. Koros, and I. Lefkovits. 1974. Plaque forming cells: methodology and theory. *Transplant. Rev.* 18:130–191.

Krause, D., S. C. Lee, and C. Deutsch. 1988. Forskolin effects on the voltage-gated K^+ conductance of human T cells. *Pfluegers Arch. Eur. J. Physiol.* 412:133–140.

Lee, J. C. R., B. Soliven, and D. J. Nelson. 1988. Beta-adrenergic stimulation modulates the activation of the voltage-dependent outward current in human T8+ lymphocytes. *Biophys. J.* 53:544*a*. (Abstr.)

Lee, S., and C. Deutsch. 1989. Temperature dependence of K^+ channel properties in lymphocytes. *Biophys. J.* 55:544*a*. (Abstr.)

Lee, S. C., D. E. Sabath, C. Deutsch, and M. B. Prystowsky. 1986. Increased voltage-gated potassium conductance during interleukin 2-stimulated proliferation of a mouse helper T lymphocyte clone. *J. Cell Biol.* 102:1200–1208.

Matteson, D. R., and C. Deutsch. 1984. K channels in T lymphocytes: a patch clamp study using monoclonal antibody adhesion. *Nature. (Lond.)*. 307:468–471.

Pahapill, P. A., and L. C. Schlichter. 1989. Effects of temperature on K^+ currents in human T-lymphocytes. *Biophys. J.* 55:8*a*. (Abstr.)

Pappone, P. A. 1980. Voltage-clamp experiments in normal and denervated mammalian skeletal muscle fibres. *J. Physiol. (Lond.)*. 306:377–410.

Parsegian, A. 1969. Energy of an ion crossing a low dielectric membrane: solutions to four relevant electrostatic problems. *Nature. (Lond.)*. 221:844–846.

Price, M., S. Lee, D. Krause, and C. Deutsch. 1988. Charybdotoxin effect on proliferation of human peripheral blood lymphocytes. *J. Cell Biol.* 107:80*a*. (Abstr.)

Schlichter, L., N. Sidell, and S. Hagiwara. 1986. Potassium channels mediate killing by human natural killer cells. *Proc. Natl. Acad. Sci. USA*. 83:451–455.

Walsh, K. B., T. B. Begenisich, and R. S. Kass. 1988. β-adrenergic modulation in the heart. Independent regulation of K and Ca channels. *Pfluegers Arch. Eur. J. Physiol.* 411:232–234.

Walsh, K. B., T. B. Begenisich, and R. S. Kass. 1989. β-adrenergic modulation of cardiac ion channels. Differential temperature sensitivity of potassium and calcium currents. *J. Gen. Physiol.* 93:841–854.

Wilson, H. A., and T. M. Chused. 1985. Lymphocyte membrane potential and Ca^{2+}-sensitive potassium channels described by oxonol dye fluorescence measurements. *J. Cell. Physiol.* 125:72–81.